Prenylated quinolinecarboxylic acid derivative prevents neuronal cell death through inhibition of MKK4

Masato Ogura[1], Haruhisa Kikuchi[2], Norshalena Shakespear[1], Toshiyuki Suzuki[1], Junko Yamaki[1], Miwako K. Homma[1], Yoshiteru Oshima[2], and Yoshimi Homma[1, *]

[1]Fukushima Medical University School of Medicine, Fukushima 960-1295, Japan

[2]Graduate School of Pharmaceutical Sciences, Tohoku University, Sendai 980-8678, Japan

[*]Corresponding author: Tel.: +81-24-5471659, Fax: +81-24-5483041, E-mail: yoshihom@fmu.ac.jp

Conflict of interest: None of the authors have any conflict of interest.

Abstract

The development of neuroprotective agents is necessary for the treatment of neurodegenerative diseases. Here, we report PQA-11, a prenylated quinolinecarboxylic acid (PQA) derivative, as a potent neuroprotectant. PQA-11 inhibits glutamate-induced cell death and caspase-3 activation in hippocampal cultures, as well as inhibits N-Methyl-4-phenylpyridinium iodide- and amyloid $\beta_{1\text{-}42}$-induced cell death in SH-SY5Y cells. PQA-11 also suppresses mitogen-activated protein kinase kinase 4 (MKK4) and c-jun N-terminal kinase (JNK) signaling activated by these neurotoxins. Quartz crystal microbalance analysis and *in vitro* kinase assay reveal that PQA-11 interacts with MKK4, and inhibits its sphingosine-induced activation. The administration of PQA-11 by intraperitoneal injection alleviates 1-methyl-4-phenyl-1,2,3,6-tetrahydropyridine-induced degeneration of nigrostriatal dopaminergic neurons in mice. These results suggest that PQA-11 is a unique MKK4 inhibitor with potent neuroprotective effects *in vitro* and *in vivo*. PQA-11 may be a valuable lead for the development of novel neuroprotectants.

Keywords

Neuronal cell death, neurodegeneration, MAPK, neurotoxin, small molecule

Chemical compounds studied in this article

Ppc-1 (PubChem CID: 46910769), PQA-18 (PubChem CID: 73602831), PQA-11 (PubChem CID: 74223691)

1. Introduction

Cell death plays a critical role in the pathology of various neurological diseases in the nervous system [1–3]. Neurotrophic factor depletion and the activation of excitatory neurotransmitter receptors trigger cell death in neurons through the activation of caspase-3 [3–8]. In addition, the accumulation of abnormal proteins including amyloid proteins and neurotoxins induce neuronal cell death, which is involved in the etiology of neurodegenerative diseases such as Alzheimer's disease (AD) and Parkinson's disease (PD) [9–11]. This cell death is modulated by highly regulated signaling pathways including mitogen-activated protein kinase (MAPK) [12,13]. c-Jun N-terminal kinase (JNK), a member of the MAPK family, is a Ser/Thr kinase activated by various stresses such as reactive oxygen species [12,13]. JNK activates the cell death pathway via phosphorylation of cellular substrates including c-Jun, a component of the transcription factor activator protein-1 [12–14]. As JNK activation is observed in some experimental models including excitotoxicity, nerve growth factor withdrawal, and ischemia [15–18], the development of novel drugs that inhibit the JNK pathway is valuable for the treatment of neuronal cell death.

Cellular slime molds are soil microorganisms that produce many pharmacologically active molecules and are an important source of lead compounds for medical research [19–21]. We previously reported that Ppc-1, a secondary metabolite containing a unique structure of prenylated quinolinecarboxylic acid (PQA), derived from *Polysphondylium pseudocandidum*, enhances mitochondrial oxygen consumption and induces weight loss in mice without lesional changes in kidney or liver tissues or tumor formation [22]. In the present study, we have synthesized a series of PQA derivatives, and selected PQA-11 as a potent neuroprotectant through the inhibition of the MKK4-JNK signaling pathway. PQA-11 inhibits MKK4 autophosphorylation and subsequently JNK activity, which prevents neuronal cell death induced by various neurotoxins. These findings suggest that PQA-11 is a novel

MKK4 inhibitor with potent neuroprotective effects.

2. Materials and methods

2.1. Antibodies and Chemicals

The PQA compounds used in this study were synthesized and purified as previously described [23,24], and the structure and purity were confirmed by ^{1}H and ^{13}C NMR spectroscopy and high-resolution mass spectroscopy. The purities of all compounds were greater than 98%. Mouse anti-β-actin monoclonal antibody (mAb), mouse anti-microtubule associated protein-2 (MAP2) mAb, dimethyl sulfoxide (DMSO), glyceryl trioctanoate, N-Methyl-4-phenylpyridinium iodide (MPP^{+}), sphingosine, SP600125 and amyloid $\beta_{1\text{-}42}$ ($A\beta_{1\text{-}42}$) were purchased from Sigma-Aldrich (St. Louis, MO); 1-methyl-4-phenyl-1,2,3,6-tetrahydropyridine (MPTP) was purchased from Tokyo Kasei Kogyo (Tokyo, Japan); rabbit anti-cleaved caspase-3 (Asp175) mAb, rabbit anti-phospho-c-Jun (Ser73) mAb, rabbit anti-phospho-JNK (Thr183/Tyr185) mAb, rabbit anti-phospho-p38 (Thr180/Tyr182) mAb, rabbit anti-phospho-MKK4 (Thr261) polyclonal antibody, rabbit anti-MKK4 polyclonal antibody, rabbit anti-phospho-ASK1 (Thr845) polyclonal antibody, rabbit anti-phospho-MLK3 (Thr277/Ser281) polyclonal antibody and rabbit anti-glial fibrillary acidic protein (GFAP) mAb were obtained from Cell Signaling Technology (Beverly, MA); Mouse anti-GST mAb was obtained from Wako (Tokyo, Japan); Mouse anti-tyrosine hydratase (TH) mAb was obtained from Merck Millipore (Billerica, MA); Rabbit anti-phospho-leucine-rich repeat kinase 2 (LRRK2) (Ser935) mAb was obtained from Abcam (Cambridge, MA). All other chemicals and reagents were of the highest grade commercially available.

2.2. Animal study

All the experiments were conducted in accordance with the guidelines of the National Institutes of Health, as well as the Ministry of Education, Culture, Sports, Science and

Technology of Japan, and were approved by the Fukushima Medical University Animal Studies Committee. All efforts were made to minimize animal suffering, to reduce the number of animals used, and to utilize alternatives to *in vivo* techniques. Male C57BL/6J mice (9-week old) were obtained from CLEA Japan (Tokyo, Japan), and housed at 21°C with a 12:12-h light/dark cycle with free access to water and a commercial diet. MPTP was used to induce Parkinsonism in animal models [25]. After preliminary breeding for one week, mice were treated with vehicle (0.1% DMSO), PQA-11 (0.5 mg/kg), or SP600125 (1.0 mg/kg) by intraperitoneal injection three times a week for two weeks. MPTP (20 mg/kg) or PBS (control) was administered four times at 2 h intervals on Day 1 of the second week [25]. Control mice received PBS only. Stock solutions of PQA-11 and SP600125 were diluted with glyceryl trioctanoate, and treatment of PQA-11 (0.5 mg/kg), SP600125 (1.0 mg/kg), or vehicle (0.1% DMSO) was started a week before the MPTP injection by intraperitoneal injection three times a week. A week after the MPTP injection, the mice were sacrificed and brain tissue was prepared for immunohistochemistry. For the assessment of glutamate-induced cell death, primary neurons were prepared from the hippocampus of 17-day-old embryonic C57BL/6J mice as described previously [26]. The embryonic hippocampus was dissected and incubated with Versene (Thermo Fisher Scientific) at room temperature for 12 min. Neurons were then mechanically dissociated with a fire-narrowed Pasteur pipette in the culture medium. Isolated neurons were plated at a density of 6.3×10^4 cells/cm^2 on wells coated with poly-D-lysine and laminin and maintained in Neurobasal medium supplemented with 2% B-27, 500 μM glutamine, 50 U/ml penicillin and 50 μg/ml streptomycin in a humidified atmosphere of 5% CO_2 and 95% air at 37°C. The neuronal cells cultivated for 11 days *in vitro* (DIV) were treated with or without glutamate at 10 μM for 24 h in the absence or presence of PQA compounds at 100 nM, and cell viability was evaluated by immunocytochemistry with anti-MAP2 antibody. The IC_{50} values for the inhibition of

glutamate-induced cell death were obtained with four different concentrations of the PQA compounds.

2.3. Immunohistochemistry

Brains were embedded in Tissue Tek (Sakura Finetek, Torrance, CA), frozen in liquid nitrogen, and stored at -80ºC. Cryostat sections (30 μm in thickness) were prepared, air-dried, and fixed in 10% neutral formaldehyde solution for 10 min. Sections were blocked with 5% swine serum (Vector Laboratories, Burlingame, CA) and stained with anti-TH mAb. Mouse antibody was detected with anti-mouse IgG conjugated with biotin (Vector Laboratories). The immunoreactive signals were visualized using a Vectastain ABC kit (Vector Laboratories) with 3,3'-diaminobenzide tetrahydrochloride/H_2O_2 as a chromogen. The number of stained cells was counted with a computer-assisted imaging program. Eight to 10 sections obtained from the individual animals were used for evaluation of the TH-positive cells.

2.4. Cell cultures

Human neuroblastoma SH-SY5Y cells (passage numbers 4-10, CRL-2266: American Type Culture Collection, Manassas, VA) were cultivated in growth medium consisting of a 1:1 mixture of MEM/Ham's F-12 supplemented with 10% (v/v) heat-inactivated fetal bovine serum (FBS, Sigma-Aldrich) in a humidified atmosphere of 5% CO_2 and 95% air at 37°C. SH-SY5Y cells are widely used as a model in studies involving neuronal injury or death, as well as neurodegenerative diseases [27]. We confirmed that MPP^+ activates caspase-3 and JNK signaling in a dose-dependent manner in undifferentiated, intact SH-SY5Y cells. $A\beta_{1-42}$ was dissolved in growth medium without FBS to make up the 100 μM stock solution and kept at -80°C. When needed for experiments, an aliquot of $A\beta_{1-42}$ solution was maintained at 37°C for 48 h to make aggregates prior to treating the cells [27]. For the assessment of cell death,

SH-SY5Y cells were treated with or without MPP^+ at 3 mM for 24 h $A\beta_{1-42}$ at 1 or 10 μMfor 48 h in the absence or presence of various concentrations of PQA-11 or SP600125 at 1 μM. Cell viabilities were evaluated by flow cytometric analysis and immunocytochemistry with anti-cleaved caspase-3 antibody.

2.5. Immunocytochemistry

The neuronal cells (11 DIV) or SH-SY5Y cells growing on glass coverslips were fixed with 10% neutral formaldehyde solution for 15 min at room temperature. The cells were permeabilized with 0.1% Triton X-100 in PBS containing 5% swine serum for 1 h at room temperature and incubated with the primary antibody overnight at 4°C. The cells were then reacted with anti-mouse IgG antibody or anti-rabbit IgG antibody conjugated with Alexa Fluor 488 (Thermo Fisher Scientific) for 1 h at room temperature, and observed under a confocal laser-scanning microscope system, FV-1000D (Olympus, Tokyo, Japan). Under the culture condition, 98% of primary hippocampal neurons were immunoreactive for the neuronal marker MAP2 on double immunocytochemistry with anti-MAP2 antibody and anti-GFAP antibody as the astroglial markers.

2.6. Immunoblotting

The neuronal cells (11 DIV) or SH-SY5Y cells were solubilized in lysis buffer (PBS, pH 7.4, 1% *n*-dodecyl-β-D-maltoside [DDM], 1 mM Na_3VO_4) containing aprotinin (10 μg/ml), leupeptin (10 μg/ml), and phenylmethylsulfonyl fluoride (1 mM). After incubating on ice for 15 min, the lysates were clarified by centrifugation at 12,000 *g* for 15 min. After protein determination by a Bio-Rad protein assay reagent (Bio-Rad Laboratories, Hercules, CA), the supernatants (20 μg) were subjected to SDS-PAGE and the proteins were transferred to PVDF filter membranes (Millipore, Billerica, MA). The membranes were blocked with 5% non-fat

dry milk in Tris-buffered saline containing 0.05% Tween 20 and incubated with primary antibodies. Blots were probed with goat anti-mouse IgG antibody or anti-rabbit IgG antibody coupled to HRP (Bio-Rad Laboratories), and the positive signals were visualized by ECL (PerkinElmer, Waltham, MA). Band intensities were quantified using Image J software (1.47V, US National Institutes of Health).

2.7. Flow cytometric analysis

To analyze activation of cellular caspase-3 and phosphorylation of c-Jun, single-cell suspensions from SH-SY5Y cells were obtained by trypsin and aliquots of cells suspensions (10^6 cells) were stained with Alexa488-conjugated anti-cleaved caspase-3 antibody and anti-phospho-c-Jun antibody, respectively. Stained cells were analyzed with FACSCanto II (BD Biosciences, San Jose, CA) as described previously [28].

2.8. In vitro kinase assay

Full-length cDNAs for human MKK4 (GenBank accession no. **NM_003010**) and human LRRK2 (GenBank accession no. **NM_198578**) were obtained by RT-PCR using total RNA from normal human lung fibroblast TIG7 cells [26], and cloned into the pGEX-4T-1. Constitutive active type of MKK4 (CA-MKK4) was produced by replacing Ser257 with Glu and Thr261 with Asp using the primeSTAR mutagenesis kit (Takara, Shiga, Japan) [29]. A GST-MKK4, GST-CA-MKK4, or GST-LRRK2 protein was expressed in *Escherichia coli* and purified with glutathione Sepharose 4B as described previously [30]. These GST proteins were incubated with or without sphingosine in a kinase buffer consisting of 20 mM Hepes-NaOH, pH7.4, 10 mM $MgCl_2$ and 200 μM ATP in a total volume of 40 μL at 30°C for 20 min as described previously [30]. Phosphorylation of the GST proteins was assessed by immunoblotting with an anti-phospho-MKK4 or anti-phospho-LRRK2 antibody.

2.9. RNA interference

The silencer select pre-designed short interfering RNA (siRNA) for human MKK4 (s12703) was obtained from Thermo Fisher Scientific. The scramble sequence for the control (5′-AGGUAGUGUAAUCGCCUUGdTdT-3′) was designed as previously described [30]. To achieve gene silencing, SH-SY5Y cells were transfected with the siRNA for 24 h using the Neon Transfection System (Thermo Fisher Scientific) according to the manufacturer's recommended protocol [31]. Under this transfection condition, we confirmed over 90% reduction in the MKK4 protein levels by immunoblotting with anti-MKK4 antibody.

2.10. Quartz crystal microbalance (QCM)

QCM was used to analyze the potential binding between PQA-11 and MKK4, CA-MKK4, or LRRK2. QCM measurement was performed using AFFINIX QN (Initium Inc., Kanagawa, Japan) [32]. Briefly, 5 μL of a mixture of H_2SO_4 and H_2O_2 (3:1, called as piranha solution) was mounted to the Au surface on the quartz crystal sensor, and incubated for 5 min at room temperature. The sensor was then washed thoroughly with distilled water, and washing was repeated three times. After the sensor was dried, it was applied with 1 μL of PQA-11 solution (10 mg/mL in DMSO), and PQA-11 immobilization was performed with incubation for 30 min at room temperature under saturated humidity. The immobilized-PQA-11 sensor was immersed in a batch cell with 5 mL PBS. A corresponding amount of samples was added into the batch cell. Changes in frequency were recorded point by point until the adsorption was saturated. The dissociation rate constant (*K*d) was calculated using AQUA software (Initium Inc.).

2.11. LC/MS/MS

Mice were treated with PQA-11 (0.5 mg/kg) by intraperitoneal single injection, brain tissues were prepared at 2, 4, and 6 h after the PQA-11 injection. PQA-11 in the brain tissues was analyzed by C18 reverse-phase liquid chromatography coupled to high resolution Mass spectrometry (MS) as described previously [22]. Briefly, PQA-11 was extracted by the method of Bligh and Dyer [33]. For detection of PQA-11, the extracts were analyzed on high performance liquid chromatography (LC)-MS/MS system (LC, UltiMate 3000; MS, TSQ Vantage and Orbitrap, Thermo Fisher Scientific) controlled by XCALIBUR. The *m/z* list of PQA-11 was obtained from Mass Frontier (version 7.0, Thermo Fisher Scientific) software for the prediction of PQA-11 fragments. The peak area of PQA-11 as a parent compound was calculated from mass spectra obtained by positive acquisition polarity in a mass spectrometer. To assess relative concentrations of PQA-11, the peak area of PQA-11 was normalized to that of quinine added as an internal standard.

2.12. Data analysis

The statistical significance of differences was determined using the one-way analysis of variance with Tukey-Kramer post-hoc comparisons. Data are expressed as mean and SD (**, $p<0.01$; *, $p<0.05$, as compared with control: $^{\#\#}$, $p<0.01$; $^{\#}$, $p<0.05$, as compared with the neurotoxins-treated group).

3. Results

3.1. Inhibition of glutamate-induced cell death by PQA-11

Since Ppc-1 exhibited neuroprotective effects on glutamate-induced cell death in hippocampal cultures (IC_{50}: 239 nM; Figs. 1A and B), we evaluated a number of PQA compounds using the hippocampal cultures, and the most potent protection was observed with PQA-11 (IC_{50}: 127 nM; Figs. 1A and B). No protective effect was detected with immunosuppressive PQA-18 (Figs. 1A and B) [24]. Thus, we chose PQA-11 for further analyses and examined the effect of PQA-11 on the activation of caspase-3, which is evident in glutamate-treated cells. The cultures were treated with glutamate for 6 h in the absence or presence of PQA-11, followed by the determination of cleaved caspase-3 protein levels. As shown in Fig. 1C, a marked increase in cleaved caspase-3 protein levels was observed in the glutamate-stimulated hippocampal cultures. PQA-11 significantly suppressed the activation of caspase-3, while PQA-11 alone did not affect cleaved caspase-3 protein levels.

3.2. Inhibition of MPP^+- and $A\beta_{1-42}$-induced cell death by PQA-11

The above results led us to examine the pharmacological profiles of PQA-11, using *in vitro* models of PD and AD, that is, SH-SY5Y human neuroblastoma cells treated with MPP^+ and $A\beta_{1-42}$, respectively [18,25,27]. The cells were treated with MPP^+ for 24 h in the absence or presence of PQA-11 or a specific JNK inhibitor SP600125, and caspase-3 activation was determined with flow cytometric analysis. MPP^+ significantly increased the number of activated caspase-3-positive cells as compared with the control in SH-SY5Y cells, and PQA-11 and SP600125 significantly suppressed it in a concentration-dependent manner [control: 22.3±2.1%; MPP^+: 52.1±3.6%**; MPP^+ + SP600125 (1 μM): 15.9%±4.8%$^{\#\#}$; MPP^+ + PQA-11 (1 nM): 41.5±2.2%$^{\#}$; MPP^+ + PQA-11 (10 nM): 29.1±3.3%$^{\#\#}$; MPP^+ + PQA-11 (100 nM):

21.5±2.1%$^{\#\#}$; **p<0.01, as compared with control; $^{\#}$p<0.05, $^{\#\#}$p<0.01, as compared with MPP^+; one-way ANOVA with Tukey-Kramer post hoc comparisons] (Fig. 2A). Similar results were obtained using immunoblotting analysis (Fig. 2B). We further studied the effects of PQA-11 on $A\beta_{1-42}$-induced cell death in SH-SY5Y cells. When cells were treated with aggregated $A\beta_{1-42}$ for 48 h in the absence or presence of PQA-11, the number of activated caspase-3-positive cells was significantly increased by treatment with aggregated $A\beta_{1-42}$, which was significantly suppressed by treatment with PQA-11 (Fig. 3A).

3.3. Inhibition of the MKK4-JNK pathway by PQA-11

JNK and MKK4 is involved in the cell death pathway and regulated by MAPKK kinase (MAPKKK) such as ASK1 [12–14,34]. To understand the inhibition mechanism of cell death by PQA-11 in SH-SY5Y cells treated with MPP^+, we examined the phosphorylation of signaling molecules of the JNK pathway. When cells were treated with MPP^+ for 30 min in the absence or presence of PQA-11, phosphorylation of c-Jun, which is a specific JNK substrate, was remarkably increased as compared with the control in SH-SY5Y cells, and PQA-11 significantly suppressed it in a concentration-dependent manner (Fig. 2C). Similar results were obtained using flow cytometric analysis (Fig. 2D). We confirmed that SP600125 significantly inhibited MPP^+- triggered phosphorylation of c-Jun (Fig. 2D). Additionally, when the cells were treated with MPP^+ for 15 min in the absence or presence of PQA-11, phosphorylation of JNK, MKK4, LRRK2, but not ASK1, MLK3, and p38, was evident in the SH-SY5Y cells (Fig. 2E). PQA-11 significantly suppressed MPP^+-triggered phosphorylation of these signaling molecules in a concentration-dependent manner (Fig. 2E), possibly suggesting that PQA-11 inhibits the MPP^+-induced LRRK2-MKK4-JNK pathway in SH-SY5Y cells. Similar results were obtained when $A\beta_{1-42}$ was used as an inducer of cell death. As shown in Figures 3B and 3C, aggregated $A\beta_{1-42}$ induced the phosphorylation of JNK and

MKK4 in a time-dependent and concentration manner, and this increase was significantly suppressed by the treatment with PQA-11 at all time points tested. These results suggest that PQA-11 inhibits cell death through JNK pathway suppression in SH-SY5Y cells treated with MPP^+ or aggregated $A\beta_{1-42}$.

The effect of MKK4 siRNA on the caspase-3 activation was tested to confirm the MKK4 requirement for the neurotoxins-induced cell death. We confirmed that the MKK4 expression level was significantly suppressed by treatment with MKK4 siRNA in SH-SY5Y cells in a dose-dependent manner. No effect was detected with the control siRNA. When the cells were introduced with MKK4 siRNA and then treated with MPP^+ for 24 h, the number of activated caspase-3-positive cells was recovered to near control levels (Fig. 4A). Similar results were obtained when aggregated $A\beta_{1-42}$ was used as a neurotoxin (Fig. 4B). These results suggest an indispensable role for MKK4 in neurotoxin-induced cell death.

3.4. Interaction of PQA-11 with MKK4

To understand the molecular basis on MKK4-JNK pathway inhibition by PQA-11, we examined the interaction of PQA-11 with MKK4, constitutive active type MKK4 (CA-MKK4), or LRRK2 using the QCM method. PQA-11 was immobilized on the Au surface on the sensor, and the frequency of Au self-oscillation was markedly diminished by adding GST-MKK4 to the assay solution, showing a strong binding of PQA-11 and MKK4 (Fig. 5A). This effect was in a concentration-dependent manner, and the *K*d values for the interaction between PQA-11 and MKK4 were calculated as 1.15×10^{-8} M (Fig. 5B). No response was detected with GST-CA-MKK4, GST-LRRK2, or GST. These results suggest that PQA-11 directly interacts with resting MKK4 rather than activated MKK4 or LRRK2.

Recent studies have suggested that sphingosine derived from ceramide is involved in the activation of the JNK pathway and subsequent cell death [35]. Thus, we examined the effect

of sphingosine on the interaction between GST-MKK4 and PQA-11 using QCM. As shown in Fig. 6A, the frequency, which was quite low when GST-MKK4 was added to the solution, was slightly restored by adding sphingosine. Sphingosine alone did not cause the frequency change, showing no direct binding of sphingosine to PQA-11. These results suggest that PQA-11 might interfere with sphingosine binding to MKK4, but not to PQA-11. Based on the previous studies on MKK4 that autophosphorylation at Thr261 is required for full kinase activity [36], GST-MKK4 solution was incubated with ATP in the absence or presence of sphingosine. As shown in Figure 6B, sphingosine itself induced the autophosphorylation of GST-MKK4 in a concentration-dependent manner, and this phosphorylation was significantly inhibited by adding PQA-11 (Fig. 6C). These results suggest that PQA-11 inhibits sphingosine-induced MKK4 autophosphorylation.

3.5. Alleviation of MPTP-induced neurodegeneration by PQA-11

The MPTP model was employed for the assessment of the neuroprotective effects of PQA-11 *in vivo* [25,34]. C57BL/6J mice were administered with MPTP to induce degeneration in nigrostriatal dopaminergic neurons, and treated with a vehicle (0.1% DMSO), PQA-11 (0.5 mg/kg) or SP600125 (1.0 mg/kg), three times a week by intraperitoneal administration. SP600125 was used as a positive control [37]. As shown in Figure 7, the number of the TH-positive cells in substantia nigra was reduced by the administration of MPTP as compared with the control, which was alleviated by the administration of PQA-11 or SP600125 (control: 334±21 cells; MPTP: 82±16 cells**; MPTP + PQA-11: 145±18 cells$^{\#\#}$; MPTP + SP600125: 142±22 cells$^{\#\#}$; **$p<0.01$, as compared with control; $^{\#\#}p<0.01$, as compared with MPTP; one-way ANOVA with Tukey-Kramer post hoc comparisons). These findings indicate that PQA-11 displays a neuroprotective effect *in vivo*. To investigate the distribution of PQA-11 in the brain, the mice were intraperitoneally administered with PQA-11 (0.5 mg/kg) and brain

extracts were examined by mass spectrometric analysis. The peaks of PQA-11 at the positions of 358.20 *m/z* and 290.14 *m/z* were confirmed as parent compound by MS and MS/MS, respectively (Figs. 8A and B). The peak at the position of 290.14 *m/z* was detected in the brain samples of individuals at 4 h and 6 h after the PQA-11 administration (Fig. 8C). These results suggest that PQA-11 is delivered to the brain after intraperitoneal administration.

4. Discussion

We demonstrated in our study that PQA-11 suppresses neurotoxin-induced cell death through MKK4-JNK signaling pathway inhibition. JNK plays a crucial role in neuronal cell death by activating the mitochondrial apoptosis pathway and subsequently activating caspase-3, an effector at the endpoint of the JNK-cell death pathway [12–18]. We detected the active form of caspase-3 in mouse hippocampal cultures treated with glutamate and human SH-SY5Y cells treated with either MPP^+ or $A\beta_{1\text{-}42}$. Additionally, PQA-11 treatment attenuated the activation of caspase-3 and cell death in all three independent experiments (Figs. 1–3). JNK is a member of the MAPK family and is activated by MAPKKs, which are regulated by MAPKKKs [12]. MAPKKKs are activated under various conditions such as cellular stress and oxidative stress [13,14]. ASK1, a member of MAPKKK family, is activated by oxidative stress, and other members of the MAPKKK family, MEKK1/4 and MLK2/3, are activated by cellular stress through small GTPases [14]. These MAPKKKs phosphorylate and activate members of MAPKKs, such as MKK4 and MKK7, which phosphorylate and activate JNK [13]. Here, we observed the activation of MKK4 in MPP^+- or $A\beta_{1\text{-}42}$-treated SH-SY5Y cells (Figs. 2 and 3). Since treatment with siMKK4 suppresses this MKK4 and caspase-3 activation (Fig. 4), MKK4 is possibly involved in the neurotoxin-derived JNK activation and cell death. Besides, PQA-11 attenuates the activity of LRRK2, a member of MAPKKK family, in addition to MKK4 (Fig. 2C). No significant changes are detected with other MAPKKKs such as ASK1 and MLK3 in MPP^+-treated SH-SY5Y cells. Taken together, the above results suggest that the LRRK2-MKK4-JNK pathway is mainly enhanced in neurotoxin-treated SH-SY5Y cells, and that PQA-11 suppresses neurotoxin-induced JNK and caspase-3 activation through affecting LRRK2 and MKK4, the upstream kinases of JNK signaling.

The action mechanism underlying the inhibition of LRRK2 and MKK4 activity by PQA-11 is interesting. Our QCM analysis and *in vitro* kinase assay reveal that sphingosine directly

interacts with MKK4 and increases its activity (Fig. 6). We also demonstrate that PQA-11 directly interacts with MKK4, but not with LRRK2. Furthermore, PQA-11 suppresses sphingosine binding to MKK4, while PQA-11 does not directly interact with sphingosine (Figs. 5 and 6). Preliminary results of the MKK4 structural analysis using Autodock Vina software [38] suggest a single, common binding pocket for PQA-11 (-6.3 kcal/mol) and sphingosine (-4.2 kcal/mol) on MKK4 (PDB structure; 3vut) [39]. MKK4 requires sphingosine binding for autophosphorylation. A recent study revealed that the Ser257 and Thr261 residues of MKK4 is required for autophosphorylation and the subsequent full activation, while only a trace of MKK4 activation is observed when these sites were replaced by alanine [36]. Thus, we speculate that PQA-11 inhibits MKK4 through interfering with the binding of sphingosine in a competitive manner. Molecular basis of LRRK2 inhibition by PQA-11 remains to be solved. On the other hand, we have previously reported that another PQA compound, PQA-18, suppresses PAK2 activity [24]. PAK is a kinase regulated by p21 GTPases, and its autophosphorylation is dependent on interacting with sphingosine [40], indicating that the molecular basis of PAK2 inhibition by PQA-18 may be similar to the case of MKK4 by PQA-11. PQA-11 does not affect kinase activity of PAK2, and PQA-18 does not affect that of MKK4 (data not shown). These findings may suggest that the PQA core structure is required to interfere with sphingosine binding to kinases.

New neuroprotectants that have a therapeutic effect and cause no adverse effects are important for the treatment for patients with neurodegenerative diseases. Recently, a number of small molecules, including recombinant proteins such as neurotrophic factors, growth factors, erythropoietin, and anti-amyloid β antibody, have also been developed for neuroprotection [41–43]. However, their clinical applications are limited by the appearance of serious side effects such as cerebral vasculitis and stroke, poor bioavailability, and low blood-brain barrier permeability [44]. Although donepezil and rivastigmine were also developed as

an acetylcholine esterase inhibitor and were approved for AD treatment and improve AD symptom but do not prevent the progression of AD because these drugs do not inhibit neuronal cell death [45]. Therefore, the development of a new drug that inhibits neuronal cell death is required for the treatment of neurodegenerative diseases. We have shown in this study that PQA-11 prevents neuronal cell death through MKK4 inhibition *in vitro* (Figs. 2 and 3). Furthermore, PQA-11 prevented MPTP-induced degeneration of nigrostriatal dopaminergic neurons *in vivo* (Fig. 7). These results imply that PQA-11 can serve as an inhibitor of neuronal cell death in the brain. We confirmed the distribution of PQA-11 in the brains of mice treated with PQA-11 administered intraperitoneally. PQA-11 was also detected as a parent compound in mouse brain extracts by using LC/MS/MS 4 h after its administration (Fig. 8), showing that it is delivered to the brain through the blood-brain barrier and may display neuroprotective activity by its direct effect on neurons. Recent studies have demonstrated that JNK inhibitors, such as SP600125, prevent MPTP-induced neuronal cell death in the substantia nigra [46]. However, JNK is expressed in various tissues including the brain, and JNK inhibitors may possess various adverse effects including immune deficiency and cancer development by affecting cell differentiation and proliferation [47,48]. In contrast, the expression of MKK4 is high in neurons but low in glial or peripheral tissues [34]. RNA-seq analysis confirms the high levels of MKK4 in the brain [49]. Thus, MKK4 inhibitor PQA-11 is expected to be a more selective neuroprotective effect than other JNK inhibitors for the treatment of neurodegenerative diseases. PQA-11 may be a useful lead compound for the development of neuroprotective drugs.

In summary, we have reported that PQA-11 is a potent inhibitor of neuronal cell death. PQA-11 inhibits MKK4 activation by interfering with sphingosine binding to MKK4, which in turn suppresses the MKK4-JNK pathway. We have further demonstrated that PQA-11 exhibits a therapeutic effect on neurodegeneration *in vivo* using the MPTP model. These

results suggest that PQA-11 may be a feasible lead compound for the development of novel neuroprotectants.

Acknowledgements

This work was funded by the Japan Society for the Promotion of Science (Grant-in-Aid for Scientific Research) and Fukushima Medical University (grant for Project Research).

References

[1] M.P. Mattson, Apoptosis in neurodegenerative disorders, Nat. Rev. Mol. Cell Biol. 1 (2000) 120-129.

[2] J. Yuan, B.A. Yankner, Apoptosis in the nervous system, Nature 407 (2000) 802-809.

[3] D.E. Bredesen, R.V Rao, P. Mehlen, Cell death in the nervous system, Nature 443 (2006) 796-802.

[4] J.T. Coyle, P. Puttfarcken, Oxidative stress, glutamate, and neurodegenerative disorders, Science 262 (1993) 689-695.

[5] D.W. Choi, Excitotoxic cell death, J. Neurobiol. 23 (1992) 1261-1276.

[6] A.B. MacDermott, M.L. Mayer, G.L. Westbrook, S.J. Smith, J.L. Barker, NMDA-receptor activation increases cytoplasmic calcium concentration in cultured spinal cord neurones, Nature 321 (1986) 519-522.

[7] R. Sattler, M. Tymianski M, Molecular mechanisms of glutamate receptor-mediated excitotoxic neuronal cell death, Mol. Neurobiol. 24 (2001) 107-129.

[8] Y, Fuchs, H. Steller, Programmed cell death in animal development and disease, Cell 147 (2011) 742-758.

[9] H. Oakley, S.L. Cole, S. Logan, E. Maus, P. Shao, J. Craft, A. Guillozet-Bongaarts, M. Ohno, et al., Intraneuronal beta-amyloid aggregates, neurodegeneration, and neuron loss in transgenic mice with five familial Alzheimer's disease mutations: potential factors in amyloid plaque formation, J. Neurosci. 26 (2006) 10129-10140.

[10] M.K. Lee, W. Stirling, Y. Xu, X. Xu, D. Qui, A.S. Mandir, T.M. Dawson, N.G. Copeland, et al., Human alpha-synuclein-harboring familial Parkinson's disease-linked Ala-53 --> Thr mutation causes neurodegenerative disease with alpha-synuclein aggregation in transgenic mice, Proc. Natl. Acad. Sci. U S A. 99 (2002) 8968-8973.

[11] D. Aarsland, B. Creese, M. Politis, K.R. Chaudhuri, D.H. Ffytche, D. Weintraub, C.

Ballard, Cognitive decline in Parkinson disease, Nat. Rev. Neurol. 13 (2017) 217-231.

[12] T. Yamasaki, H. Kawasaki, H. Nishina, Diverse Roles of JNK and MKK Pathways in the Brain, J. Signal. Transduct. (2012) 459265.

[13] X. Wang, A. Destrument, C. Tournier, Physiological roles of MKK4 and MKK7: insights from animal models, Biochim. Biophys. Acta. 1773 (2007) 1349-1357.

[14] Z. Xu, A.C. Maroney, P. Dobrzanski, N.V. Kukekov, L.A. Greene, The MLK family mediates c-Jun N-terminal kinase activation in neuronal apoptosis, Mol. Cell Biol. 21 (2001) 4713-4724.

[15] C. Centeno, M. Repici, J.Y. Chatton, B.M. Riederer, C. Bonny, P. Nicod, M. Price, P.G. Clarke, et al., Role of the JNK pathway in NMDA-mediated excitotoxicity of cortical neurons, Cell Death. Differ. 14 (2007) 240-253.

[16] J. Ham, A. Eilers, J. Whitfield, S.J. Neame, B. Shah, c-Jun and the transcriptional control of neuronal apoptosis, Biochem. Pharmacol. 60 (2000) 1015-1021.

[17] T.W. Lai, S. Zhang, Y.T. Wang, Excitotoxicity and stroke: identifying novel targets for neuroprotection, Prog. Neurobiol. 115 (2014) 157-188.

[18] A. Sclip, X. Antoniou, A. Colombo, G.G. Camici, L. Pozzi, D. Cardinetti, M. Feligioni, P. Veglianese, et al., c-Jun N-terminal kinase regulates soluble Aβ oligomers and cognitive impairment in AD mouse model, J. Biol. Chem. 286 (2011) 43871-43880.

[19] H.R. Morris, G.W. Taylor, M.S. Masento, K.A. Jermyn, R.R. Kay, Chemical structure of the morphogen differentiation inducing factor from Dictyostelium discoideum, Nature 328 (1987) 811-814.

[20] Y. Kubohara, H. Kikuchi, Y. Matsuo, Y. Oshima, Y. Homma, Mitochondria are the target organelle of differentiation-inducing factor-3, an anti-tumor agent isolated from Dictyostelium Discoideum, PLoS. One. 8 (2013) e72118.

[21] Y. Kubohara, H. Kikuchi, Y. Matsuo, Y. Oshima, Y. Homma, Properties of a non-

bioactive fluorescent derivative of differentiation-inducing factor-3, an anti-tumor agent found in Dictyostelium discoideum, Biol. Open. 3 (2014) 289-296.

[22] T. Suzuki, H. Kikuchi, M. Ogura, M.K. Homma, Y. Oshima, Y. Homma, Weight loss by Ppc-1, a novel small-molecule mitochondrial uncoupler derived from slime mold, PLoS. One. 10 (2015) e0117088.

[23] H. Kikuchi, T. Suzuki, M. Ogura, M.K. Homma, Y. Homma, Y. Oshima, Synthesis of prenylated quinolinecarboxylic acid derivatives and their anti-obesity activities, Bioorg. Med. Chem. 23 (2015) 66-72.

[24] M. Ogura, H. Kikuchi, T. Suzuki, J. Yamaki, M.K. Homma, Y. Oshima, Y. Homma, Prenylated quinolinecarboxylic acid derivative suppresses immune response through inhibition of PAK2, Biochem. Pharmacol. 105 (2016) 55-65.

[25] C.M. Chong, D. Ma, C. Zhao, R.J. Franklin, Z.Y. Zhou, N. Ai, C. Li, H. Yu, et al., Discovery of a novel neuroprotectant, BHDPC, that protects against MPP+/MPTP-induced neuronal death in multiple experimental models, Free Radic. Biol. Med. 89 (2015) 1057-1066.

[26] M. Ogura, J. Yamaki, M.K. Homma, Y. Homma, Mitochondrial c-Src regulates cell survival through phosphorylation of respiratory chain components, Biochem. J. 447 (2012) 281-289.

[27] N. Hettiarachchi, M. Dallas, M. Al-Owais, H. Griffiths, N. Hooper, J. Scragg, J. Boyle, C. Peers, Heme oxygenase-1 protects against Alzheimer's amyloid-β(1-42)-induced toxicity via carbon monoxide production, Cell Death. Dis. 5 (2014) e1569.

[28] M. Ogura, T. Inoue, J. Yamaki, M.K. Homma, T. Kurosaki, Y. Homma, Mitochondrial reactive oxygen species suppress humoral immune response through reduction of CD19 expression in B cells in mice, Eur. J. Immunol. 47 (2017) 406-418.

[29] Z. Guan, S.Y. Buckman, B.W. Miller, L.D. Springer, A.R. Morrison. Interleukin-1beta-

induced cyclooxygenase-2 expression requires activation of both c-Jun NH2-terminal kinase and p38 MAPK signal pathways in rat renal mesangial cells, J. Biol. Chem. 273 (1998) 28670-28676.

[30] M. Ogura, J. Yamaki, M.K. Homma, Y. Homma, Phosphorylation of flotillin-1 by mitochondrial c-Src is required to prevent the production of reactive oxygen species, FEBS. Lett. 588 (2014) 2837-2843.

[31] A. Anitha, I. Thanseem, K. Nakamura, M.M. Vasu, K. Yamada, T. Ueki, Y. Iwayama, T. Toyota, et al., Zinc finger protein 804A (ZNF804A) and verbal deficits in individuals with autism, J. Psychiatry Neurosci. 39 (2014) 294-303.

[32] H. Matsuno, H. Furusawa, Y. Okahata, Kinetic studies of DNA cleavage reactions catalyzed by an ATP-dependent deoxyribonuclease on a 27-MHz quartz-crystal microbalance, Biochemistry 44 (2005) 2262-2270.

[33] E.G. Bligh, W.J. Dyer, A rapid method of total lipid extraction and purification, Can. J. Biochem. Physiol. 37 (1959) 911-917.

[34] M.S. Saporito, B.A. Thomas, R.W. Scott, MPTP activates c-Jun NH(2)-terminal kinase (JNK) and its upstream regulatory kinase MKK4 in nigrostriatal neurons in vivo, J. Neurochem. 75 (2000) 1200-1208.

[35] M.M. Young, M. Kester, H.G. Wang, Sphingolipids: regulators of crosstalk between apoptosis and autophagy, J. Lipid Res. 54 (2013) 5-19.

[36] K. Deacon, J.L. Blank, Characterization of the mitogen-activated protein kinase kinase 4 (MKK4)/c-Jun NH2-terminal kinase 1 and MKK3/p38 pathways regulated by MEK kinases 2 and 3. MEK kinase 3 activates MKK3 but does not cause activation of p38 kinase in vivo, J. Biol. Chem. 272 (1997) 14489-14496.

[37] B.L. Bennett, D.T. Sasaki, B.W. Murray, E.C. O'Leary, S.T. Sakata, W. Xu, J.C. Leisten, A. Motiwala, et al., SP600125, an anthrapyrazolone inhibitor of Jun N-terminal kinase,

Proc. Natl. Acad. Sci. U S A. 98 (2001) 13681-13686.

[38] C.F. Le, M.Y. Yusof, M.A. Hassan, V.S. Lee, D.M. Isa, S.D. Sekaran, In vivo efficacy and molecular docking of designed peptide that exhibits potent antipneumococcal activity and synergises in combination with penicillin, Sci. Rep. 5 (2015) 11886.

[39] T. Matsumoto, T. Kinoshita, Y. Kirii, T. Tada, A. Yamano, Crystal and solution structures disclose a putative transient state of mitogen-activated protein kinase kinase 4, Biochem. Biophys. Res. Commun. 425 (2012) 195-200.

[40] G.M. Bokoch, A.M. Reilly, R.H. Daniels, C.C. King, A. Olivera, S. Spiegel, U.G. Knaus, A GTPase-independent mechanism of p21-activated kinase activation. Regulation by sphingosine and other biologically active lipids, J. Biol. Chem. 273 (1998) 8137-8144.

[41] D. Ostrowski, R. Heinrich, Alternative Erythropoietin Receptors in the Nervous System, J. Clin. Med. 7(2018) E24.

[42] B. Moghaddam, J.H. Krystal, Capturing the angel in "angel dust": twenty years of translational neuroscience studies of NMDA receptor antagonists in animals and humans, Schizophr. Bull. 38 (2012) 942-949.

[43] S.A. Lipton, Paradigm shift in neuroprotection by NMDA receptor blockade: memantine and beyond, Nat. Rev. Drug Discov. 5 (2006) 160-170.

[44] H. Qosa, D.S. Miller, P. Pasinelli, D. Trotti, Regulation of ABC efflux transporters at blood-brain barrier in health and neurological disorders, Brain Res. 1628 (2015) 298-316.

[45] R. Khoury, J. Rajamanickam, G.T. Grossberg, An update on the safety of current therapies for Alzheimer's disease: focus on rivastigmine, Ther. Adv. Drug Saf. 9 (2018) 171-178.

[46] W.Wang, L. Shi, Y. Xie, C. Ma, W. Li, X. Su, S. Huang, R. Chen, et al., SP600125, a new JNK inhibitor, protects dopaminergic neurons in the MPTP model of Parkinson's disease, Neurosci. Res. 48 (2004) 195-202.

[47] C. Dong, D.D. Yang, C. Tounier, A.J. Whitmarsh, J. Xu, R.J. Davis, R.A. Flavell, JNK is required for effector T-cell function but not for T-cell activation, Nature 405 (2000) 91-94.

[48] C. Bubici, S. Papa, JNK signalling in cancer: in need of new, smarter therapeutic targets, Br. J. Pharmacol. 171 (2014) 24-37.

[49] L. Fagerberg, B.M. Hallström, P. Oksvold, C. Kampf, D. Djureinovic, J. Odeberg, M. Habuka, S. Tahmasebpoor, et al., Analysis of the human tissue-specific expression by genome-wide integration of transcriptomics and antibody-based proteomics, Mol. Cell Proteomics. 13 (2014) 397-406.

Figure legends

Figure 1. Effect of PQA-11 on glutamate-induced cell death in hippocampal cultures. (A) Structures of Ppc-1, PQA-11, and PQA-18. (B) Neuronal viability was determined by immunocytochemistry with anti-MAP2 antibody (green). The representative micrographs and the IC_{50} values of PQA compounds for the inhibition of glutamate-induced cell death are shown. Scale bar, 200 μm. (C) The activation of caspase-3 was determined by immunoblotting with anti-cleaved caspase-3 and anti-β-actin. Hippocampal cultures were treated with or without glutamate for 6 h in the absence or presence of PQA-11. The quantitative data of the ratios of cleaved caspase-3 versus β-actin are shown on the right. Data are pooled from three independent experiments and shown as mean and SD. $^{**}p<0.01$, as compared with control; $^{\#\#}p<0.01$, as compared with the glutamate-treated group (one-way ANOVA/Tukey-Kramer post-hoc comparisons).

Figure 2. Effect of PQA-11 on MPP^+-induced cell death in human SH-SY5Y cells. Activation of caspase-3 was analyzed by flow cytometric analysis (A) and immunoblotting (B). SH-SY5Y cells were treated with or without MPP^+ in the absence or presence of various concentrations of PQA-11or SP600125.The quantitative data of the ratios of cleaved caspase-3 versus β-actin are drawn in the below (B). Phosphorylation of c-Jun was analyzed by immunoblotting (C) and flow cytometric analysis (D). The cells were treated with or without MPP^+ in the absence or presence of PQA-11 at indicated concentrations or SP600125. The representative images and the quantitative data of the ratios of phosphorylated c-Jun versus β-actin are shown. (E) Phosphorylation of signaling molecules was analyzed by immunoblotting. The representative images and the quantitative data of the ratios of phosphorylated proteins versus β-actin are shown. Data are from a single experiment

representative of three independent experiments. $^{**}p<0.01$, $^{*}p<0.05$, as compared with control; $^{\#\#}p<0.01$, $^{\#}p<0.05$, as compared with the MPP^+-treated group (one-way ANOVA/Tukey-Kramer post-hoc comparisons).

Figure 3. Effect of PQA-11 on aggregated $A\beta_{1-42}$-induced cell death in human SH-SY5Y cells

(A) Activation of caspase-3 was analyzed by immunocytochemistry with anti-cleaved caspase-3 antibody (green) and Hoechst33342 (blue; Nuclei). SH-SY5Y cells were treated with or without aggregated $A\beta_{1-42}$ for 48 h in the absence or presence of PQA-11. The representative micrographs and quantitative data of the number of activated caspase-3-positive cells are shown. Scale bar, 100 μm. (B) Phosphorylated JNK and MKK4 were analyzed by immunoblotting. The cells were treated with $A\beta_{1-42}$ for indicated times in the absence or presence of PQA-11, and the cell lysates were examined by immunoblotting with indicated antibodies. The representative images and the quantitative data of the ratios of phosphorylated JNK or MKK4 versus β-actin are shown. (C) The cells were treated with $A\beta_{1-42}$ for 48 h in the absence or presence of PQA-11, and the cell lysates were examined by immunoblotting with anti-phospho-MKK4 antibody. Anti-β-actin antibody was used as reference (bottom). The representative images and the quantitative data of the ratios of phosphorylated MKK4 versus β-actin are shown. Data are pooled from three independent experiments and shown as mean and SD. $^{**}p<0.01$, as compared with the control group; $^{\#\#}p<0.01$, as compared with the $A\beta_{1-42}$-treated group (one-way ANOVA/Tukey-Kramer post-hoc comparisons).

Figure 4. Requirement of MKK4 for MPP^+- and $A\beta_{1-42}$-induced cell death in human SH-SY5Y cells.

(A) MKK4 protein levels were diminished by MKK4 siRNA. Cell lysates were prepared from SH-SY5Y cells treated with either MKK4 siRNA or control siRNA at indicated doses. The representative images and the quantitative data of the ratios of MKK4 versus β-actin are shown. (B) Activation of caspase-3 was analyzed by immunocytochemistry with anti-cleaved caspase-3 antibody (green) and Hoechst33342 (blue; Nuclei). The cells were treated with 40 pmol MKK4 siRNA (lower) or control siRNA (upper) in the absence or presence of either MPP^+ for 24 h (left) or aggregated $A\beta_{1\text{-}42}$ for 48 h (right). The representative micrographs are shown. Scale bar, 100 μm. Data are from a single experiment representative of three independent experiments. $^{**}p<0.01$, as compared with the control group (one-way ANOVA/Tukey-Kramer post-hoc comparisons).

Figure 5. Interaction of PQA-11 with MKK4 *in vitro*.

(A) Frequency change by molecular interaction. PQA-11 was immobilized on the QCM electrode and incubated with various concentrations of recombinant proteins at the time points indicated by the arrows, and time courses of the frequency change are shown. Data are from a single experiment representative of three independent experiments. (B) Dose curve of frequency change for PQA-11 immobilized on the QCM electrode in response to recombinant MKK4.

Figure 6. Effect of sphingosine on interaction of MKK4 with PQA-11 and autophosphorylation of MKK4.

(A) Frequency changes in response to the GST-MKK4 protein and sphingosine binding. PQA-11 immobilized on the QCM electrode was incubated with the GST-MKK4 proteins to reach saturation, followed by the addition of sphingosine. Representative time courses of frequency change for PQA-11 immobilized on the QCM electrode are shown. Sphingosine at indicated

concentrations was injected at the time points indicated by the arrows. (B and C) *In vitro* kinase assay were carried out using recombinant MKK4. The autophosphorylation of MKK4 at Thr261 was determined by immunoblotting with anti-phospho-MKK4 antibody. Anti-GST antibody was used as reference (bottom). The representative images and the quantitative data of the ratios of phosphorylated MKK4 versus GST are shown. Data are from a single experiment representative of three independent experiments. $^{**}p<0.01$, as compared with control; $^{\#\#}p<0.01$, as compared with the sphingosine-treated group (one-way ANOVA/Tukey-Kramer post-hoc comparisons).

Figure 7. Effect of PQA-11 on MPTP-induced degeneration of nigrostriatal dopaminergic neurons in mice.

Mice were treated with vehicle (0.1% DMSO), PQA-11 (0.5 mg/kg), or SP600125 (1.0 mg/kg) by intraperitoneal injection three times a week for two weeks. MPTP or PBS (control) was administered four times at 2 h intervals on Day 1 of the second week. TH-positive cells in the substantia nigra were determined by immunohistochemistry with anti-TH antibody. Representative images were shown (left panel: magnification ×10, scale bar, 200 μm; right panel: magnification ×40, scale bar, 100 μm). Data are from a single experiment representative of three independent experiments with four mice per group.

Figure. 8. Distribution of PQA-11 in the mouse brain tissue.

(A) Prediction of PQA-11 fragmentation. (B) PQA-11 was analyzed on LC/MS/MS. The peaks of PQA-11 at the positions of 358.20 *m/z* and 290.14 *m/z* were shown in MS spectrum (upper) and MS/MS spectrum (lower). (C) Detection of PQA-11 in brain. The brain tissues were collected from mice at the time points after intraperitoneal administration of PQA-11 (0.5 mg/kg), and the extracts were prepared and analyzed on LC/MS/MS. The quantitative

data of the ratios of the peak area of PQA-11 versus that of quinine (internal control) were shown. Data are from a single experiment representative of three independent experiments with three mice per group.

A

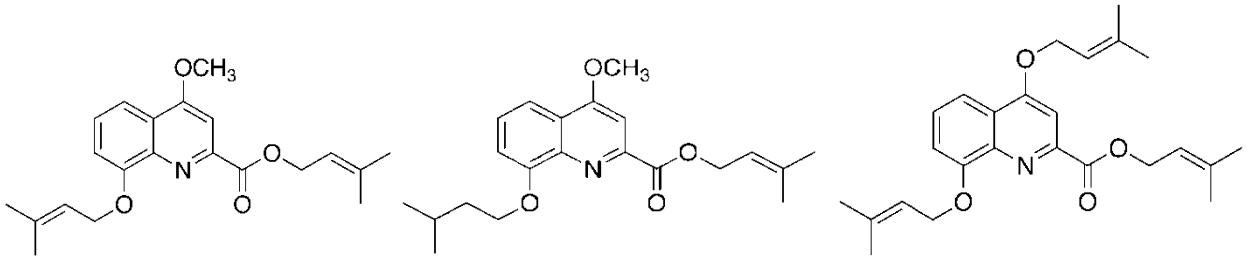

Ppc-1 PQA-11 PQA-18

B

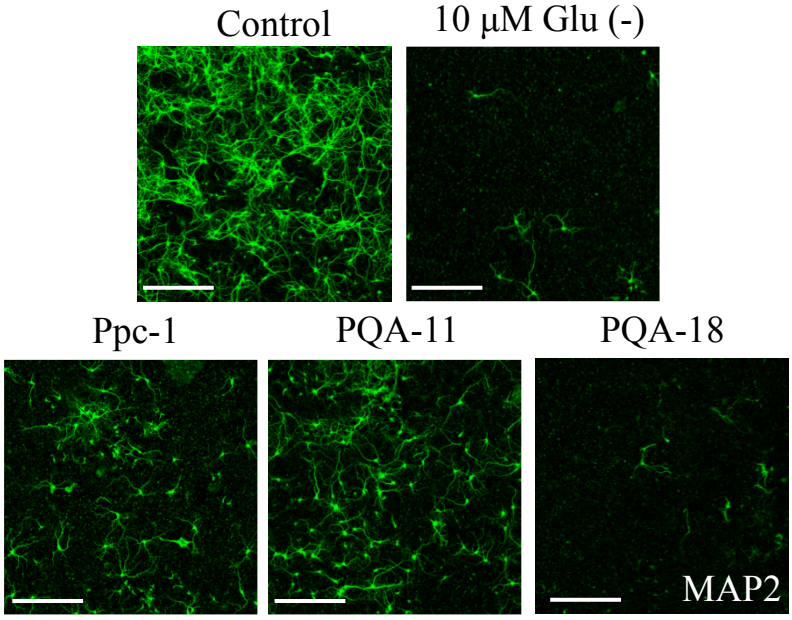

PQA compounds	IC_{50} (nM)
1 (Ppc-1)	239
7	>1000
8	314
9	>1000
11	127
12	>1000
13	>1000
14	288
16	>1000
17	>1000
18	>1000
19	>1000
20	>1000

C

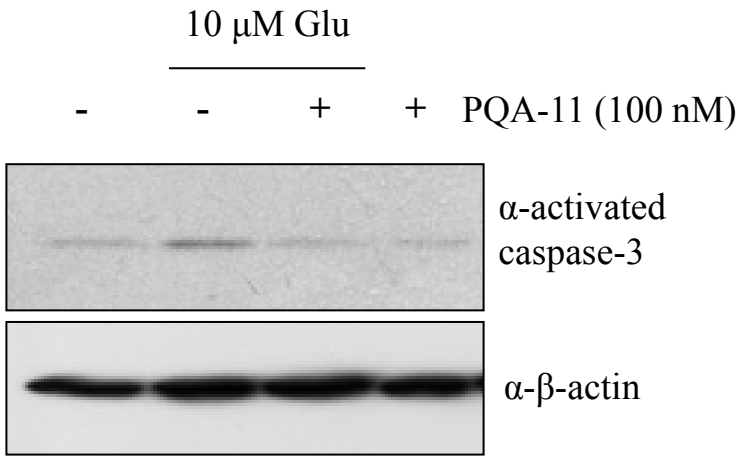

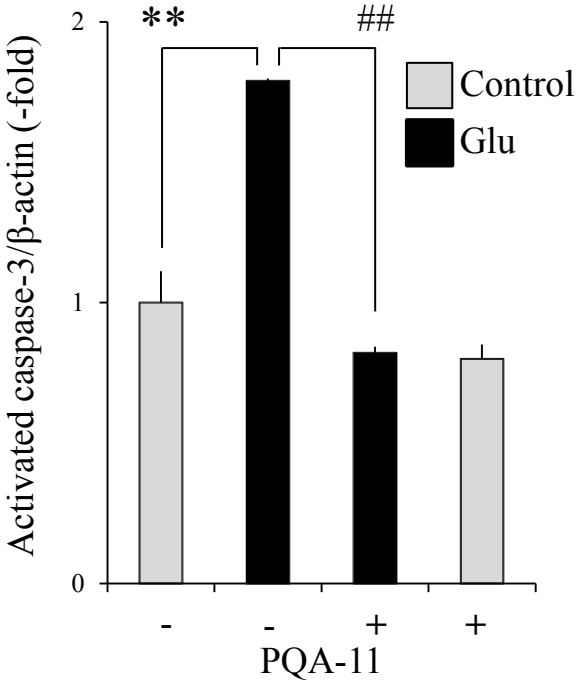

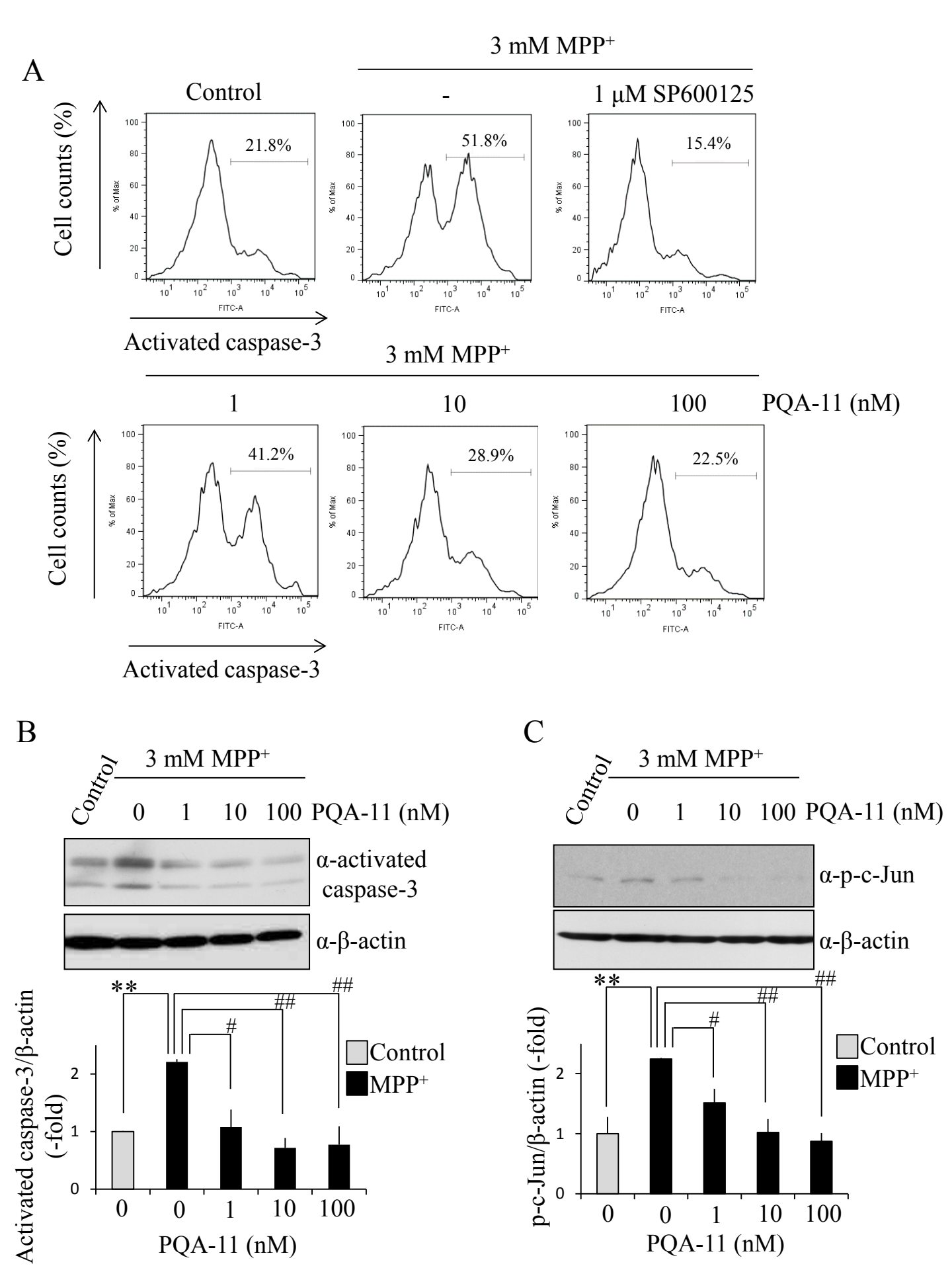
A
3 mM MPP+
Control
-
1 μM SP600125
Cell counts (%)
21.8%
51.8%
15.4%
% of Max
FITC-A
Activated caspase-3
3 mM MPP+
1
10
100
PQA-11 (nM)
41.2%
28.9%
22.5%
B
Control
3 mM MPP+
0 1 10 100 PQA-11 (nM)
α-activated caspase-3
α-β-actin
Activated caspase-3/β-actin (-fold)
**
##
#
Control
MPP+
0 0 1 10 100
PQA-11 (nM)
C
Control
3 mM MPP+
0 1 10 100 PQA-11 (nM)
α-p-c-Jun
α-β-actin
p-c-Jun/β-actin (-fold)
**
##
#
Control
MPP+
0 0 1 10 100
PQA-11 (nM)

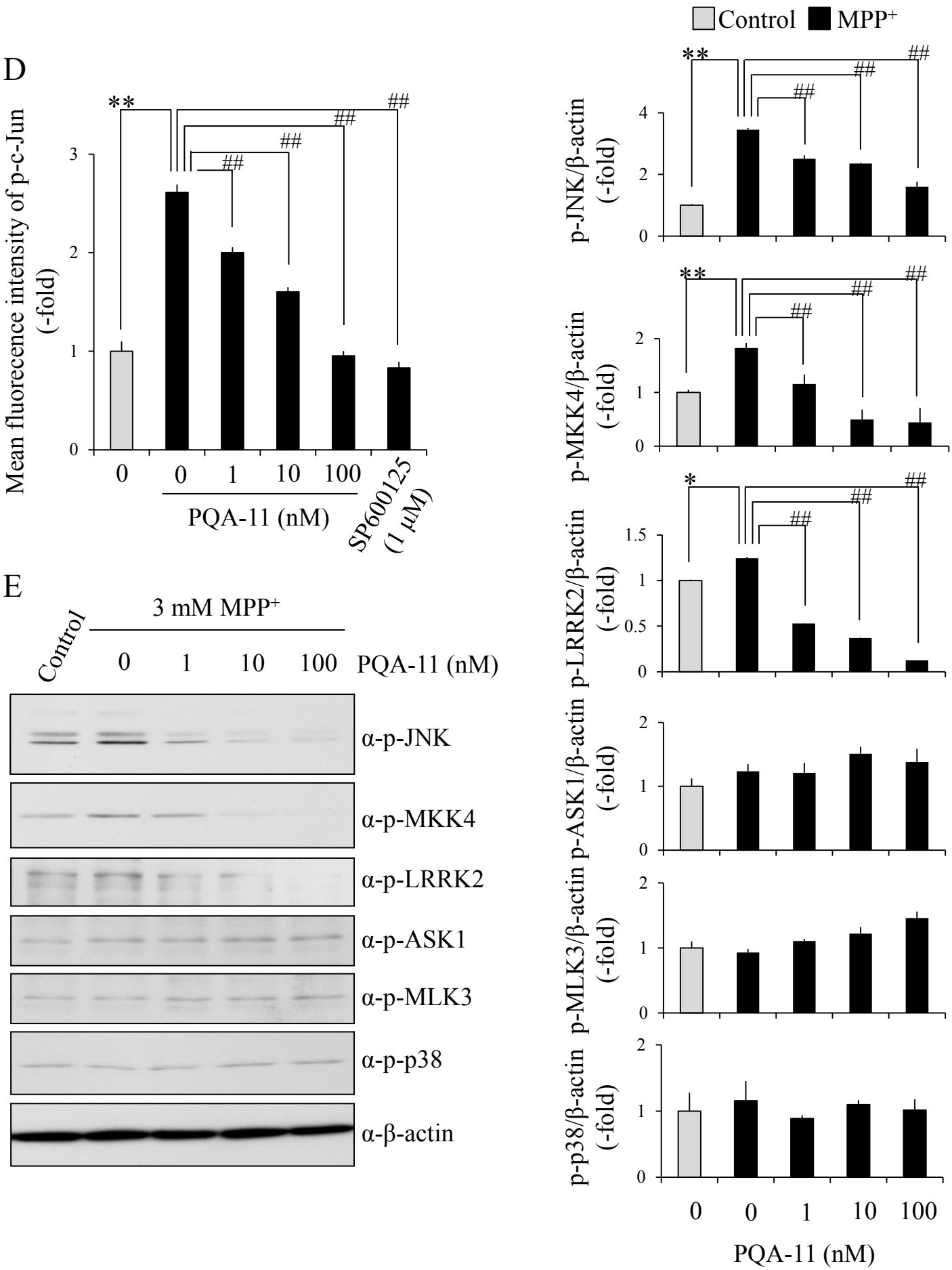
D
Mean fluorecence intensity of p-c-Jun (-fold)
**
##
0
0
1
10
100
PQA-11 (nM)
SP600125 (1 μM)
Control
MPP+
p-JNK/β-actin (-fold)
p-MKK4/β-actin (-fold)
p-LRRK2/β-actin (-fold)
p-ASK1/β-actin (-fold)
p-MLK3/β-actin (-fold)
p-p38/β-actin (-fold)
PQA-11 (nM)
E
Control
3 mM MPP+
0
1
10
100
PQA-11 (nM)
α-p-JNK
α-p-MKK4
α-p-LRRK2
α-p-ASK1
α-p-MLK3
α-p-p38
α-β-actin

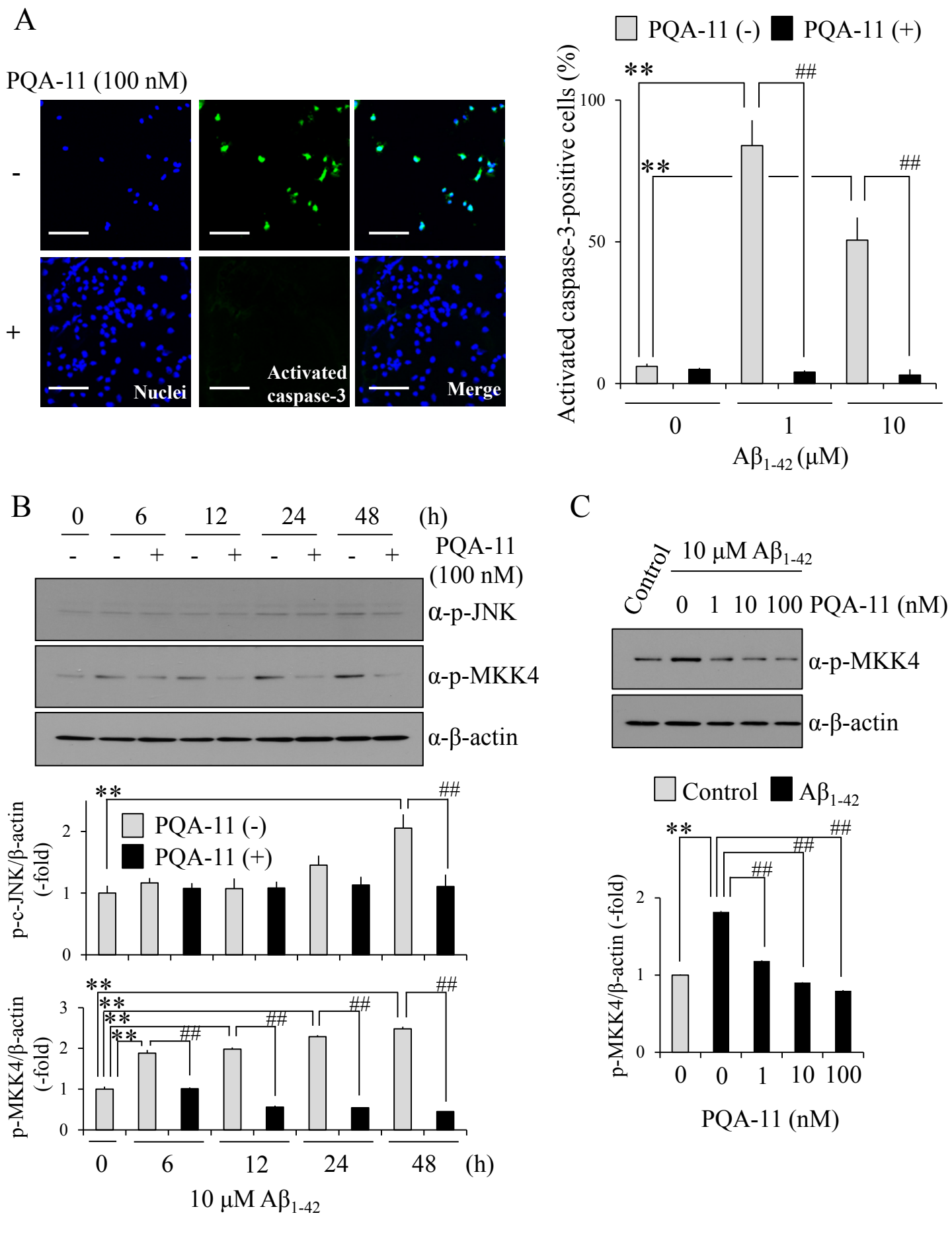
A
PQA-11 (100 nM)
-
+
Nuclei
Activated caspase-3
Merge
PQA-11 (-)
PQA-11 (+)
Activated caspase-3-positive cells (%)
100
50
0
**
**
##
##
0
1
10
Aβ1-42 (μM)
B
0
6
12
24
48
(h)
PQA-11 (100 nM)
α-p-JNK
α-p-MKK4
α-β-actin
p-c-JNK/β-actin (-fold)
PQA-11 (-)
PQA-11 (+)
p-MKK4/β-actin (-fold)
10 μM Aβ1-42
C
Control
10 μM Aβ1-42
0 1 10 100 PQA-11 (nM)
α-p-MKK4
α-β-actin
Control
Aβ1-42
p-MKK4/β-actin (-fold)
0 0 1 10 100
PQA-11 (nM)

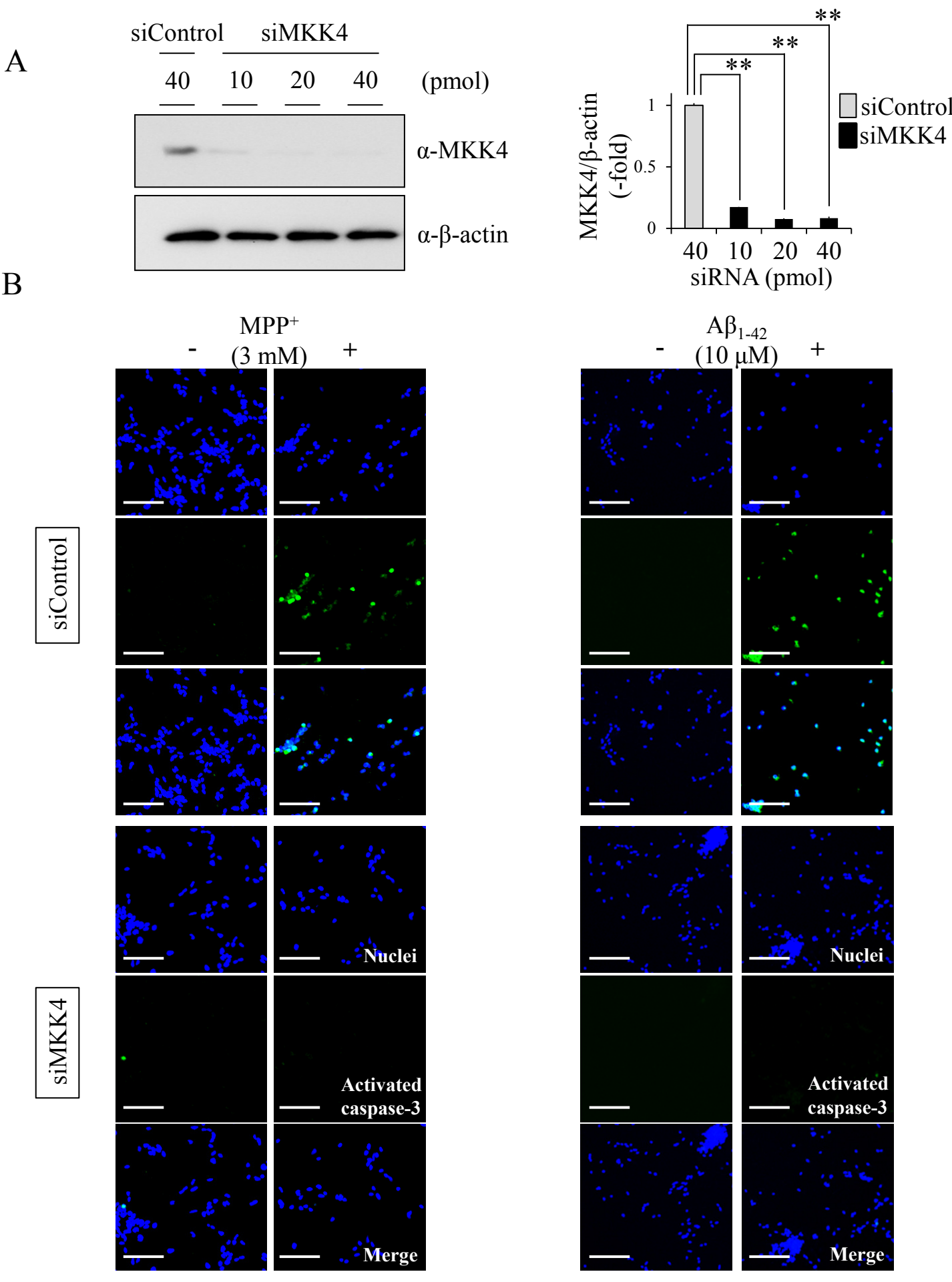
A
siControl
siMKK4
40
10
20
40
(pmol)
α-MKK4
α-β-actin
MKK4/β-actin
(-fold)
1
0.5
0
**
**
**
siControl
siMKK4
40
10
20
40
siRNA (pmol)
B
MPP+
(3 mM)
-
+
Aβ1-42
(10 μM)
-
+
siControl
siMKK4
Nuclei
Activated
caspase-3
Merge
Nuclei
Activated
caspase-3
Merge

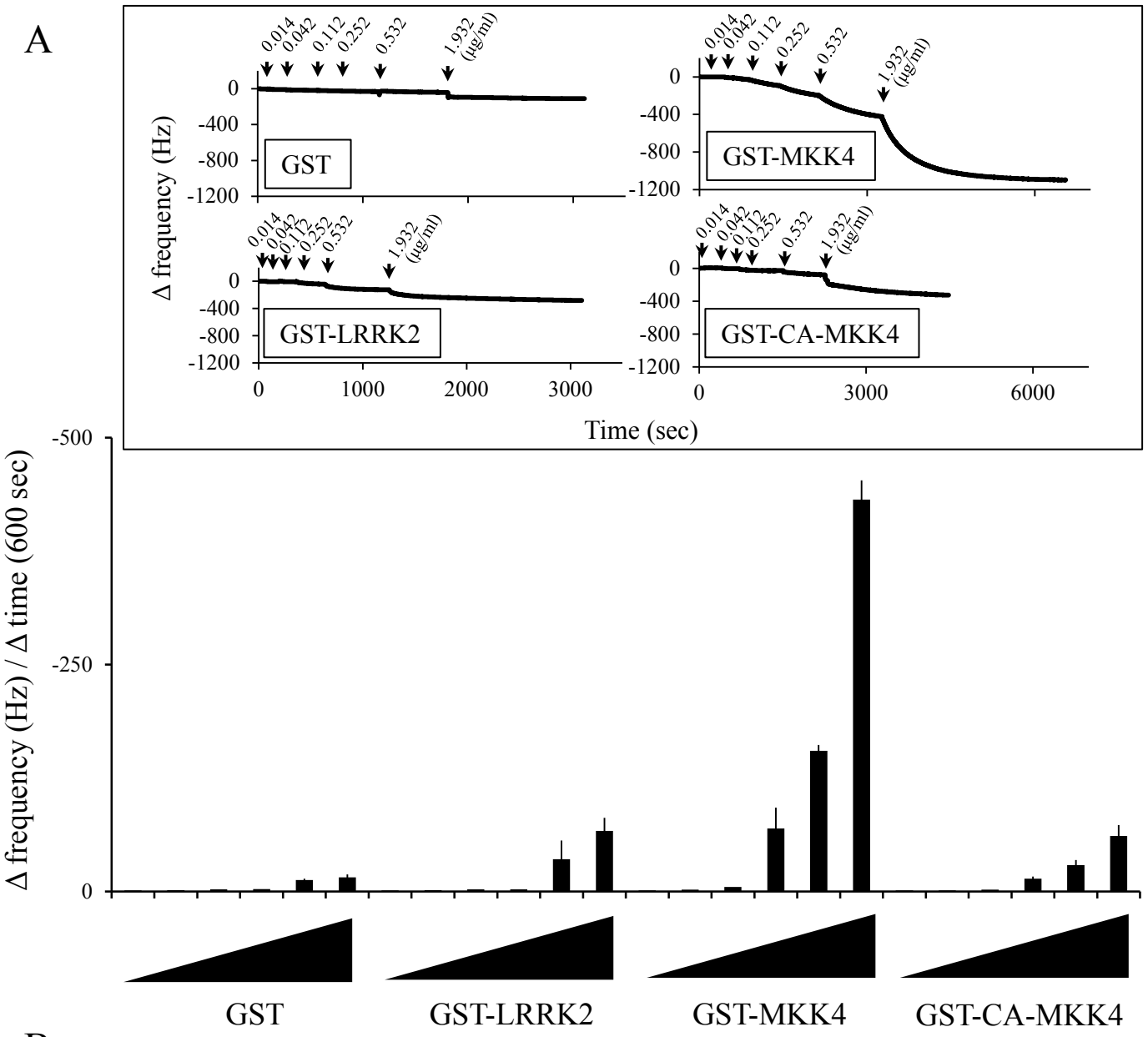
A
0.014
0.042
0.112
0.252
0.532
1.932
(μg/ml)
GST
GST-MKK4
GST-LRRK2
GST-CA-MKK4
Δ frequency (Hz)
Time (sec)
Δ frequency (Hz) / Δ time (600 sec)
GST
GST-LRRK2
GST-MKK4
GST-CA-MKK4
B
Δ frequency (Hz)
GST-MKK4 concentraion (M)

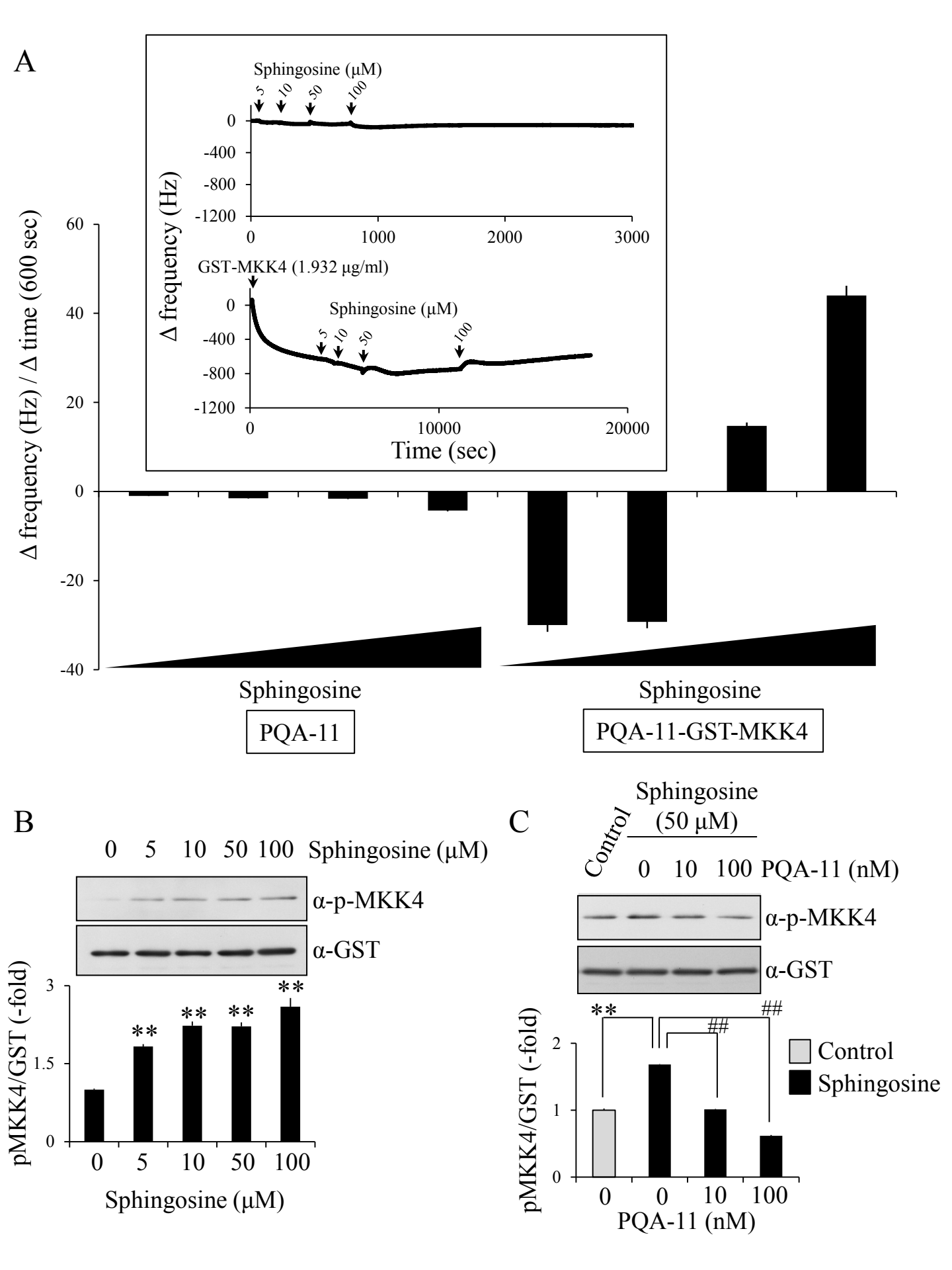
A
Sphingosine (μM)
5
10
50
100
0
-400
-800
-1200
0
1000
2000
3000
GST-MKK4 (1.932 μg/ml)
Sphingosine (μM)
5
10
50
100
0
-400
-800
-1200
0
10000
20000
Time (sec)
Δ frequency (Hz)
Δ frequency (Hz) / Δ time (600 sec)
60
40
20
0
-20
-40
Sphingosine
PQA-11
Sphingosine
PQA-11-GST-MKK4
B
0 5 10 50 100 Sphingosine (μM)
α-p-MKK4
α-GST
pMKK4/GST (-fold)
3
1.5
0
**
**
**
**
0 5 10 50 100
Sphingosine (μM)
C
Control
Sphingosine (50 μM)
0 10 100 PQA-11 (nM)
α-p-MKK4
α-GST
pMKK4/GST (-fold)
2
1
0
**
##
##
Control
Sphingosine
0 0 10 100
PQA-11 (nM)

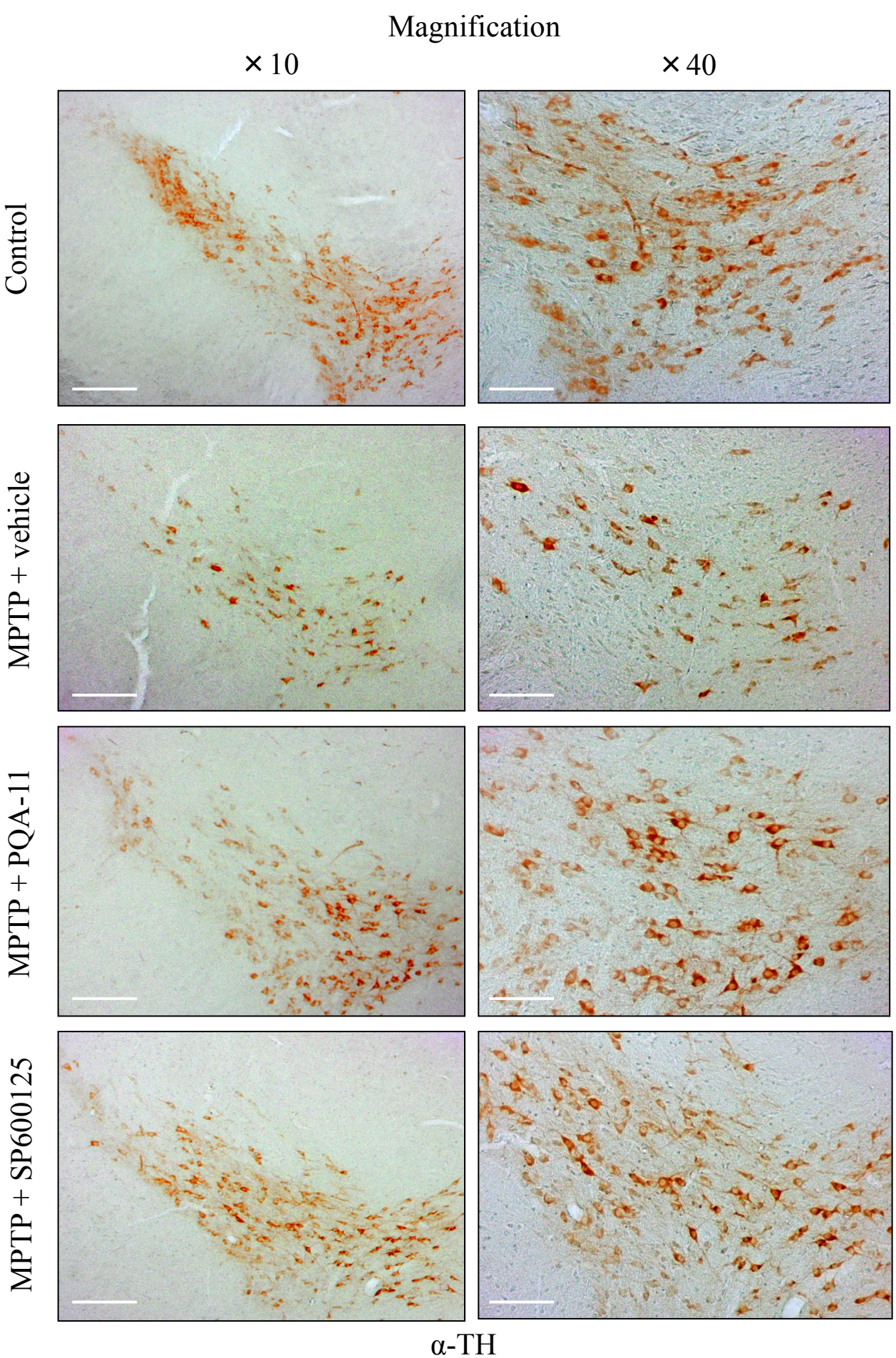
Magnification
× 10
× 40
Control
MPTP + vehicle
MPTP + PQA-11
MPTP + SP600125
α-TH

A

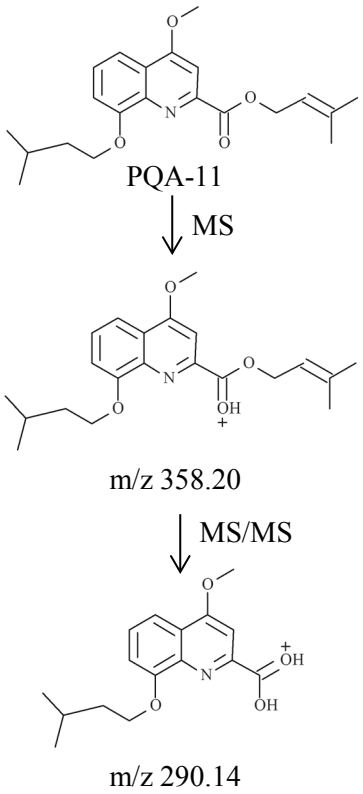
PQA-11
MS
m/z 358.20
MS/MS
m/z 290.14

C

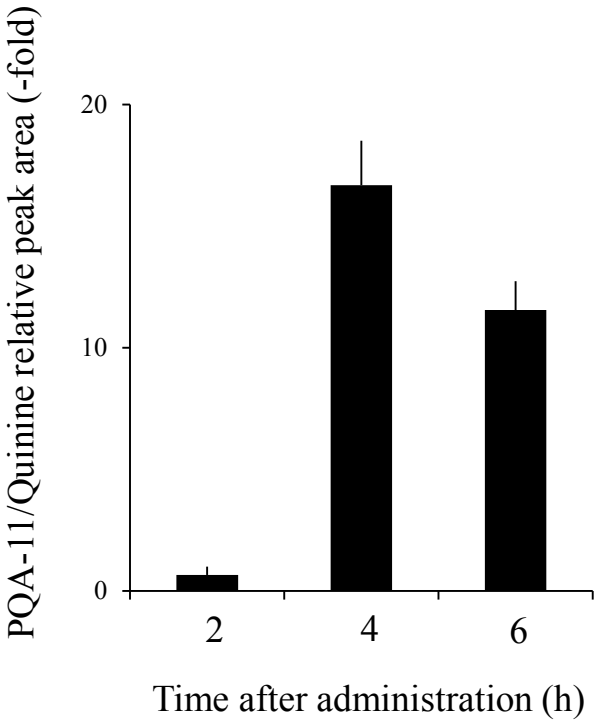
PQA-11/Quinine relative peak area (-fold)
20
10
0
2
4
6
Time after administration (h)

B

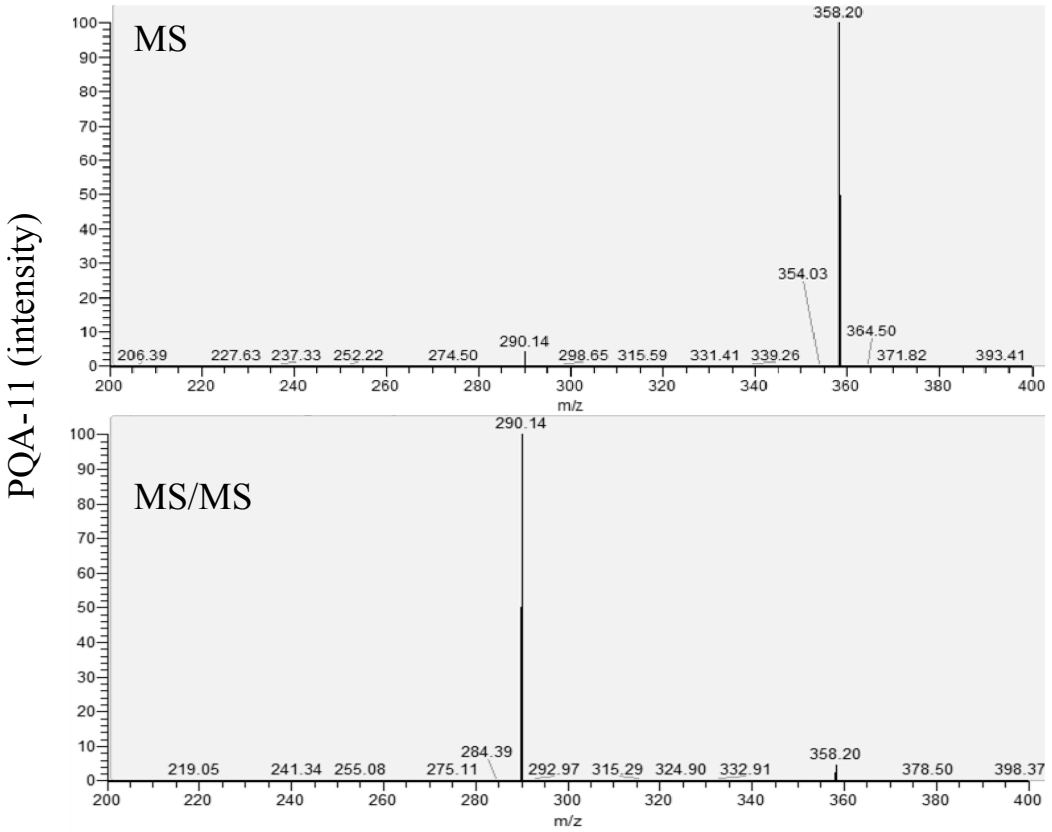
PQA-11 (intensity)
MS
358.20
354.03
364.50
290.14
206.39
227.63
237.33
252.22
274.50
298.65
315.59
331.41
339.26
371.82
393.41
m/z
MS/MS
290.14
284.39
358.20
219.05
241.34
255.08
275.11
292.97
315.29
324.90
332.91
378.50
398.37
m/z